Phys. Status Solidi A **214**, No. 7, 1700207 (2017) / **DOI** 10.1002/pssa.201700207

physica status solidi a
www.pss-a.com
applications and materials science

# Silicon self-interstitial properties deduced from platinum profiles after annealing with controlled cooling

**Anna Johnsson,**[*,1] **Peter Pichler,**[1,2] **and Gerhard Schmidt**[3]

[1] Fraunhofer Institute for Integrated Systems and Device Technology, Schottkystrasse 10, 91058 Erlangen, Germany
[2] Chair of Electron Devices, University of Erlangen–Nuremberg, Cauerstrasse 6, 91058 Erlangen, Germany
[3] Infineon Technologies Austria AG, Siemensstrasse 2, 9500 Villach, Austria

Received 22 March 2017, revised 4 April 2017, accepted 6 April 2017
Published online 6 June 2017

**Keywords** controlled cooling, diffusion, platinum, self-interstitials, silicon

[*] Corresponding author: e-mail anna.johnsson@iisb.fraunhofer.de, Phone: +49-9131 761-279, Fax: +49-9131 761-212

Experiments of platinum diffusion in silicon were used to extract information about the equilibrium concentration of silicon self-interstitials. In these experiments, the platinum was driven in from a silicide and the temperature was ramped down with different rates after the main annealing process at constant temperature. Simulations show that the concentration of substitutional platinum in the bulk region is sensitive to the value of the equilibrium concentration of self-interstitials within a certain range. It was therefore possible to determine an upper limit for that parameter at 830 °C based on our measurements.



**1 Introduction** Platinum introduces energy levels in silicon which are sufficiently deep to act as efficient recombination centers for minority charge carriers. On the other hand, since they are also sufficiently separated from midgap, they do not act as efficient generation centers as well. Both properties make platinum an ideal candidate for lifetime engineering of silicon power devices with low leakage currents.

Diffusion of platinum in silicon is known to proceed via interactions with intrinsic point defects and several authors have investigated this topic [1–4]. In an attempt to find a common parameter set for the industrially relevant processes associated with platinum diffusion, we found that some of the experiments could be described only within a certain range of self-interstitial-related parameters. The subsequent dedicated investigation lead to the suggestion of an upper limit for the self-interstitial equilibrium concentration at 830 °C presented here.

Recently, Badr et al. [4] investigated the time dependence of platinum diffusion profiles after thermal processing and were able to deduce from these experiments an upper limit for the self-interstitial equilibrium concentration in the temperature range from 730 to 950 °C. In our work, we use independent experiments to deduce the upper limit from the profile change during controlled cooling at the end of the drive-in process. Both investigations contribute new aspects to the long-lasting, but now nearly stalled debate, about the properties of intrinsic point defects, for which suggestions still exist which differ by up to ten orders of magnitude for some temperatures [5].

The experiments used in our work have been previously used by Badr et al. [4] to investigate how different cooling rates after the main annealing process affect the concentration of substitutional platinum close to the surface. From that, they could draw conclusions about the properties of vacancies. Here, we completed this work by investigating the effects of different cooling rates on the platinum profiles in the bulk of the samples.

**2 Experimental** Dislocation-free (100)-oriented, n-type phosphorus-doped, FZ-grown silicon wafers with a resistivity of 2.1 Ω cm and a thickness of 400 μm were used for the experiments. First, an oxidation step was performed (at 1000 °C for 90 min) to eliminate grown-in vacancies. The oxide was removed before the platinum was deposited onto the wafers. Prior to the drive-in step, a platinum silicide layer was formed at one surface by annealing at 500 °C. The wafers were then loaded into the furnace at 700 °C in an oxygen

ambient and the temperature was ramped up to 830 °C with an approximate rate of 8.3 K min$^{-1}$. After annealing at 830 °C for 30 min, the ambient was changed to nitrogen for another 90 min at 830 °C. The temperature was then ramped down to 700 °C after which the wafers were pulled out of the furnace. Four different ramping-down rates were used: 4.6, 2.3, 1.2, and 0.6 K min$^{-1}$.

The concentration of substitutional platinum was measured with DLTS (deep level transient spectroscopy) with an accuracy of approximately 30% [1], using a Hera–DLTS systems from PhysTech. The DLTS samples were beveled to cover the complete depth of the wafer. The preparation consisted of lapping, polishing, a wet chemical etch, HF–dip, and annealing to dissolve Pt-H complexes. Details for each step can be found in Ref. [4].

## 3 The theory of platinum diffusion

**3.1 The simulation model** Platinum is a hybrid element in silicon. It diffuses as interstitial atoms and resides mainly at substitutional sites. The transition between interstitial and substitutional sites has been modeled according to the Frank–Turnbull [6] and the kick-out [7] mechanisms. The Frank–Turnbull mechanism postulates that interstitial platinum ($Pt_i$) becomes substitutional ($Pt_s$) by reacting with vacancies (V). This can be described by the quasi-chemical reaction

$$\mathrm{Pt_i} + \mathrm{V} \underset{k_{\mathrm{FT}_\leftarrow}}{\overset{k_{\mathrm{FT}_\rightarrow}}{\rightleftharpoons}} \mathrm{Pt_s} \tag{1}$$

In parallel, the kick-out mechanism

$$\mathrm{Pt_i} \underset{k_{\mathrm{KO}_\leftarrow}}{\overset{k_{\mathrm{KO}_\rightarrow}}{\rightleftharpoons}} \mathrm{Pt_s} + \mathrm{I} \tag{2}$$

postulates that interstitial platinum goes to substitutional sites by displacing silicon lattice atoms to interstitial positions (I). Finally, bulk recombination of vacancies and self-interstitials is considered in the form

$$\mathrm{I} + \mathrm{V} \underset{k_{\mathrm{IV}_\leftarrow}}{\overset{k_{\mathrm{IV}_\rightarrow}}{\rightleftharpoons}} \emptyset \tag{3}$$

The symbol $\emptyset$ denotes the undisturbed lattice. $k_{\mathrm{FT}}$, $k_{\mathrm{KO}}$, and $k_{\mathrm{IV}}$ denote the reaction rate constants and the arrows indicate the directions. The reaction rate constants can be expressed according to Waite's theory [8] assuming diffusion-limited reactions

$$k_{\mathrm{FT}_\rightarrow} = 4\pi\, a_{\mathrm{FT}}\, (D_{\mathrm{Pt_i}} + D_{\mathrm{V}}) \tag{4}$$

$$k_{\mathrm{KO}_\leftarrow} = 4\pi\, a_{\mathrm{KO}}\, (D_{\mathrm{I}} + D_{\mathrm{Pt_s}}) \tag{5}$$

$$k_{\mathrm{IV}_\rightarrow} = 4\pi\, a_{\mathrm{IV}}\, (D_{\mathrm{I}} + D_{V}) \tag{6}$$

Therein, the $D$'s denote the diffusion coefficients of the species involved. $D_{\mathrm{Pt_s}}$ is set to 0 since substitutional platinum is assumed to be immobile. $a_{\mathrm{FT}}$, $a_{\mathrm{KO}}$, and $a_{\mathrm{IV}}$ represent the reaction radii of the respective reactions. The reaction rate constants in the reverse directions can be expressed via the concentrations in equilibrium denoted as $C^{\mathrm{eq}}$ according to

$$k_{\mathrm{FT}_\leftarrow} = k_{\mathrm{FT}_\rightarrow} C^{\mathrm{eq}}_{\mathrm{Pt_i}} C^{\mathrm{eq}}_{\mathrm{V}} / C^{\mathrm{eq}}_{\mathrm{Pt_s}} \tag{7}$$

$$k_{\mathrm{KO}_\rightarrow} = k_{\mathrm{KO}_\leftarrow} C^{\mathrm{eq}}_{\mathrm{Pt_s}} C^{\mathrm{eq}}_{\mathrm{I}} / C^{\mathrm{eq}}_{\mathrm{Pt_i}} \tag{8}$$

$$k_{\mathrm{IV}_\leftarrow} = k_{\mathrm{IV}_\rightarrow} C^{\mathrm{eq}}_{\mathrm{I}} C^{\mathrm{eq}}_{\mathrm{V}} \tag{9}$$

A system of partial differential equations can be constructed directly from Eqs. 1−3. [5]

$$\begin{aligned}\frac{\partial C_{\mathrm{Pt_s}}}{\partial t} = {} & k_{\mathrm{FT}_\rightarrow} C_{\mathrm{Pt_i}} C_{\mathrm{V}} - k_{\mathrm{FT}_\leftarrow} C_{\mathrm{Pt_s}} \\ & + k_{\mathrm{KO}_\rightarrow} C_{\mathrm{Pt_i}} - k_{\mathrm{KO}_\leftarrow} C_{\mathrm{Pt_s}} C_{\mathrm{I}}\end{aligned} \tag{10}$$

$$\begin{aligned}\frac{\partial C_{\mathrm{Pt_i}}}{\partial t} = {} & \mathrm{div}(D_{\mathrm{Pt_i}}\ \mathrm{grad}\ C_{\mathrm{Pt_i}}) \\ & - k_{\mathrm{FT}_\rightarrow} C_{\mathrm{Pt_i}} C_{\mathrm{V}} + k_{\mathrm{FT}_\leftarrow} C_{\mathrm{Pt_s}} \\ & - k_{\mathrm{KO}_\rightarrow} C_{\mathrm{Pt_i}} + k_{\mathrm{KO}_\leftarrow} C_{\mathrm{Pt_s}} C_{\mathrm{I}}\end{aligned} \tag{11}$$

$$\begin{aligned}\frac{\partial C_{\mathrm{I}}}{\partial t} = {} & \mathrm{div}(D_{\mathrm{I}}\ \mathrm{grad}\ C_{\mathrm{I}}) \\ & + k_{\mathrm{KO}_\rightarrow} C_{\mathrm{Pt_i}} - k_{\mathrm{KO}_\leftarrow} C_{\mathrm{Pt_s}} C_{\mathrm{I}} \\ & - k_{\mathrm{IV}_\rightarrow} C_{\mathrm{I}} C_{\mathrm{V}} + k_{\mathrm{IV}_\leftarrow}\end{aligned} \tag{12}$$

$$\begin{aligned}\frac{\partial C_{\mathrm{V}}}{\partial t} = {} & \mathrm{div}(D_{\mathrm{V}}\ \mathrm{grad}\ C_{\mathrm{V}}) \\ & - k_{\mathrm{FT}_\rightarrow} C_{\mathrm{Pt_i}} C_{\mathrm{V}} + k_{\mathrm{FT}_\leftarrow} C_{\mathrm{Pt_s}} \\ & - k_{\mathrm{IV}_\rightarrow} C_{\mathrm{I}} C_{\mathrm{V}} + k_{\mathrm{IV}_\leftarrow}\end{aligned} \tag{13}$$

The surfaces are assumed to be able to establish equilibrium for I and V. Accordingly, Dirichlet boundary conditions with the respective equilibrium concentrations were used for $C_{\mathrm{I}}$ and $C_{\mathrm{V}}$ at both surfaces. The surface with the PtSi layer was approximated as an infinite source maintaining interstitial platinum at its equilibrium concentration $C^{\mathrm{eq}}_{\mathrm{Pt_i}}$ via a Dirichlet boundary condition. A Neumann boundary condition was used for $C_{\mathrm{Pt_i}}$ at the other side since no interaction with the surface is assumed there.

The initial conditions depend on the substrate material. In our case, the wafer saw an oxidation step to eliminate grown-in vacancies before platinum was introduced. $C_{\mathrm{V}}$ was therefore assumed to be initially small. $C_{\mathrm{Pt_s}}$ and $C_{\mathrm{Pt_i}}$ were

**Table 1** The simulation parameters.

| parameter | value |
|---|---|
| $C_{\mathrm{Pt_s}}^{\mathrm{eq}}$ | $5.7\times10^{24}\ \exp(-2.212\ \mathrm{eV}/kT)\ \mathrm{cm}^{-3}$ |
| $C_{\mathrm{Pt_i}}^{\mathrm{eq}}$ | $8.7\times10^{19}\ \exp(-1.87\ \mathrm{eV}/kT)\ \mathrm{cm}^{-3}$ |
| $D_{\mathrm{Pt_i}}$ | $8.33\times10^{1}\ \exp(-1.23\ \mathrm{eV}/kT)\ \mathrm{cm}^2/\mathrm{s}$ |
| $C_{\mathrm{I}}^{\mathrm{eq}} D_{\mathrm{I}}$ | $4.095\times10^{25}\ \exp(-4.82\ \mathrm{eV}/kT)\ \mathrm{cm}^{-1}\mathrm{s}^{-1}$ |
| $C_{\mathrm{V}}^{\mathrm{eq}} D_{\mathrm{V}}$ | $9.75\times10^{24}\ \exp(-4.64\ \mathrm{eV}/kT)\ \mathrm{cm}^{-1}\mathrm{s}^{-1}$ |
| $C_{\mathrm{V}}^{\mathrm{eq}}$ | $7.5\times10^{22}\ \exp(-2.556\ \mathrm{eV}/kT)\ \mathrm{cm}^{-3}$ |
| $a_{\mathrm{FT}}$ | 5.0 Å |
| $a_{\mathrm{KO}}$ | 5.0 Å |
| $a_{\mathrm{IV}}$ | 5.0 Å |

chosen to be $1\times10^8\ \mathrm{cm}^{-3}$. This is several orders of magnitude lower than the final concentrations and does not affect them. The initial concentration of self-interstitial has a minor impact on the simulation results, considering values up to $C_{\mathrm{I}}^{\mathrm{eq}}$ at 830 °C. A concentration close to 0 was used in the simulations.

The simulation model was implemented in and solved by the general purpose solver PROMIS [9].

**3.2 Parameters** The parameters used in this work are listed in Table 1. The transport capacities for vacancies ($C_{\mathrm{V}}^{\mathrm{eq}} D_{\mathrm{V}}$) and self-interstitials ($C_{\mathrm{I}}^{\mathrm{eq}} D_{\mathrm{I}}$) were taken from Südkamp and Bracht [10]. These values are based on recent measurements of the self-diffusion at low temperatures. The value for $C_{\mathrm{V}}^{\mathrm{eq}}$ was taken from Badr et al. [4] and $D_{\mathrm{V}}$ was calculated from the transport capacity.

The equilibrium concentration of substitutional platinum $C_{\mathrm{Pt_s}}^{\mathrm{eq}}$ was taken from Badr et al. [4], based on measurements made by Zimmermann [1] and their own work. The product $C_{\mathrm{Pt_i}}^{\mathrm{eq}} D_{\mathrm{Pt_i}}$ was determined experimentally by Lerch et al. [11]. The individual parameters of $C_{\mathrm{Pt_i}}^{\mathrm{eq}}$ and $D_{\mathrm{Pt_i}}$ used by Badr et al. [4] were also used in this work. Finally, as in [4], the reaction radii were all set to 5 Å.

The value of $C_{\mathrm{I}}^{\mathrm{eq}}$ at 830 °C was varied between $1\times10^5$ and $3.6\times10^{11}\ \mathrm{cm}^{-3}$ in the simulations. The latter value was suggested by Badr et al. [4] as upper limit from the time evolution of platinum profiles. $D_{\mathrm{I}}$ was adjusted so that the transport capacity remained unchanged. The activation energy of $C_{\mathrm{I}}^{\mathrm{eq}}$ was assumed to be 3.18 eV, as in Ref. [4]. Variations between 2.9 and 4.7 eV did not have a significant impact on the simulation results.

## 4 Results and discussion

**4.1 The influence of $C_{\mathrm{I}}^{\mathrm{eq}}$** The magnitude of $C_{\mathrm{I}}^{\mathrm{eq}}$ was found in the simulations to have an effect on the $\mathrm{Pt_s}$ concentration in the bulk after the temperature is ramped down to 700 °C. Two examples are depicted in Fig. 1. Small values of $C_{\mathrm{I}}^{\mathrm{eq}}$ ($1\times10^8\ \mathrm{cm}^{-3}$ in Fig. 1a) give rather flat U-shaped profiles. Larger values ($2\times10^{11}\ \mathrm{cm}^{-3}$ in Fig. 1b) result in U-shaped profiles that lightly taper down towards a lower center point. The simulations also show that differences due to the ramping-down rates are more visible for larger values of $C_{\mathrm{I}}^{\mathrm{eq}}$.

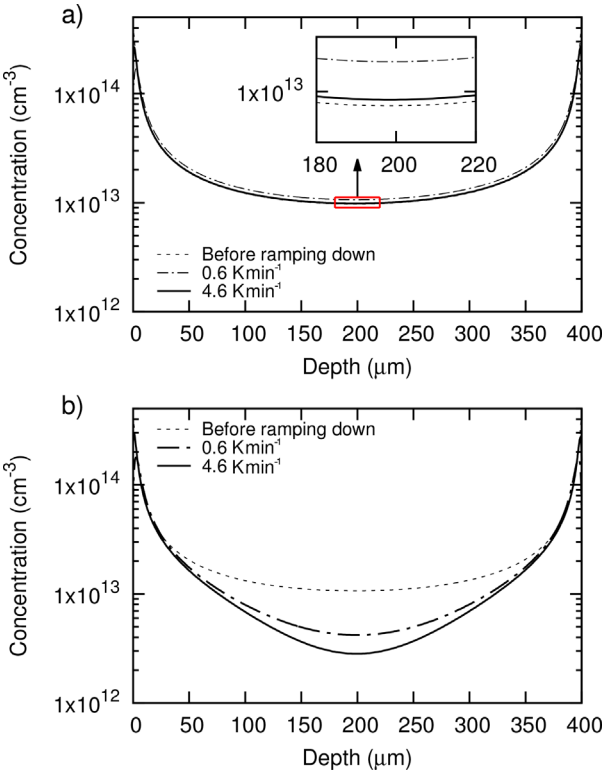


**Figure 1** Simulation results of the $\mathrm{Pt_s}$ concentration after annealing with ramping-down rates of (- — -) 0.6 K min$^{-1}$ and (——) 4.6 K min$^{-1}$ and $C_{\mathrm{I}}^{\mathrm{eq}}$ values at 830 °C of a) $1\times10^8\ \mathrm{cm}^{-3}$ and b) $2\times10^{11}\ \mathrm{cm}^{-3}$. The dashed lines (- - -) show the simulated concentration just before the temperature is ramped down.

The kick-out mechanism is dominating in the bulk region during ramping down for our conditions. The respective reaction rates in the forward and backward direction exceed the reaction rates of the Frank–Turnbull mechanism by about one order of magnitude. At the same time, the change in $C_{\mathrm{I}}$ due to bulk recombination is negligible because of the low vacancy concentration. Considering that $C_{\mathrm{Pt_i}}$ can be approximated as $C_{\mathrm{Pt_i}}^{\mathrm{eq}}$, because of the high transport capacity of interstitial platinum, a simplification of Eqs. 10 and 12 can be derived in the form

$$\frac{\partial C_{\mathrm{Pt_s}}}{\partial t} \approx k_{\mathrm{KO}_{\leftarrow}} \left( C_{\mathrm{Pt_s}}^{\mathrm{eq}}\, C_{\mathrm{I}}^{\mathrm{eq}} - C_{\mathrm{Pt_s}} C_{\mathrm{I}} \right) \tag{14}$$

$$\frac{\partial C_{\mathrm{I}}}{\partial t} \approx \mathrm{div}(D_{\mathrm{I}}\ \mathrm{grad}\ C_{\mathrm{I}}) + k_{\mathrm{KO}_{\leftarrow}} \left( C_{\mathrm{Pt_s}}^{\mathrm{eq}}\, C_{\mathrm{I}}^{\mathrm{eq}} - C_{\mathrm{Pt_s}} C_{\mathrm{I}} \right) \tag{15}$$

The diffusion term in Eq. 15 may be ignored at first based on the flat concentration profile in the bulk. The equilibrium concentrations $C_{\mathrm{Pt_s}}^{\mathrm{eq}}$ and $C_{\mathrm{I}}^{\mathrm{eq}}$ in Eqs. 14 and 15 follow Arrhenius laws and will decrease with decreasing temperature. The kick-out mechanism in the backward direction will therefore dominate during ramping down ($C_{\mathrm{Pt_s}}^{\mathrm{eq}}\, C_{\mathrm{I}}^{\mathrm{eq}} < C_{\mathrm{Pt_s}} C_{\mathrm{I}}$). The

absolute change in concentration will be the same for both $C_I$ and $C_{Pt_s}$ since self-interstitials and substitutional platinum react pairwise to interstitial platinum. However, the relative change will be much smaller for $C_{Pt_s}$ when $C_I \ll C_{Pt_s}$. The situation becomes different as soon as $C_I$ approaches $C_{Pt_s}$. The change in concentration will then have a similar impact on both $C_I$ and $C_{Pt_s}$, and the reduction of the concentration of substitutional platinum in the bulk will be more visible.

At the onset of ramping down, steady state can be assumed in the bulk so that $C_I$ is related to $C_I^{eq}$ by

$$C_I = C_I^{eq} C_{Pt_s}^{eq} / C_{Pt_s} \tag{16}$$

A large value of $C_I^{eq}$ gives a large $C_I$, which, in turn, gives a larger reduction of $C_{Pt_s}$ in the bulk after ramping down. This is confirmed by the simulations depicted in Fig. 1, where a reduction of $C_{Pt_s}$ is visible only for the larger $C_I^{eq}$ (Fig. 1b).

It is necessary to consider the diffusion term of Eq. 15 to explain further details of the simulation results. $C_I$ in the bulk will decrease as self-interstitials migrate to the surfaces. A larger decrease in $C_I$ due to out-diffusion from the bulk to the surfaces will result in a smaller reaction rate of the kick-out mechanism in the reverse direction, and a smaller impact on $C_{Pt_s}$. The change in $C_I$ is determined by the transport capacity of the self-interstitials, which is independent of the individual value of $C_I^{eq}$ since $C_I^{eq} D_I$ is kept constant. However, the relative change in $C_I$ will be larger when $C_I$ is small.

Figure 1a shows the simulation results for a small value of $C_I^{eq}$. The results show a small increase of $C_{Pt_s}$ in the bulk compared to before ramping down. The reason for this is that the out-diffusion of I's weakens the kick-out reaction in the reverse direction so that the kick-out mechanism in the forward direction is dominating during ramping down. The slower ramping-down rate gives a higher concentration since the out-diffusion operates for a longer time at higher temperatures.

The reduction of $C_{Pt_s}$ in the bulk is smaller for the slower ramping-down rate of 0.6 K min$^{-1}$ in Fig. 1b. As before, this can be explained by a weakening of the kick-out mechanism in reverse direction by the out-diffusion of I's. The effect will be larger for slower ramping-down rates since the out-diffusion operates again for a longer time at higher temperatures.

**4.2 An upper limit for $C_I^{eq}$** The measurement results are compared to the simulation results for different values of $C_I^{eq}$ at 830 °C in Fig. 2. The experiments show a rather flat concentration in the bulk region and that the ramping-down rate has an insignificant impact.

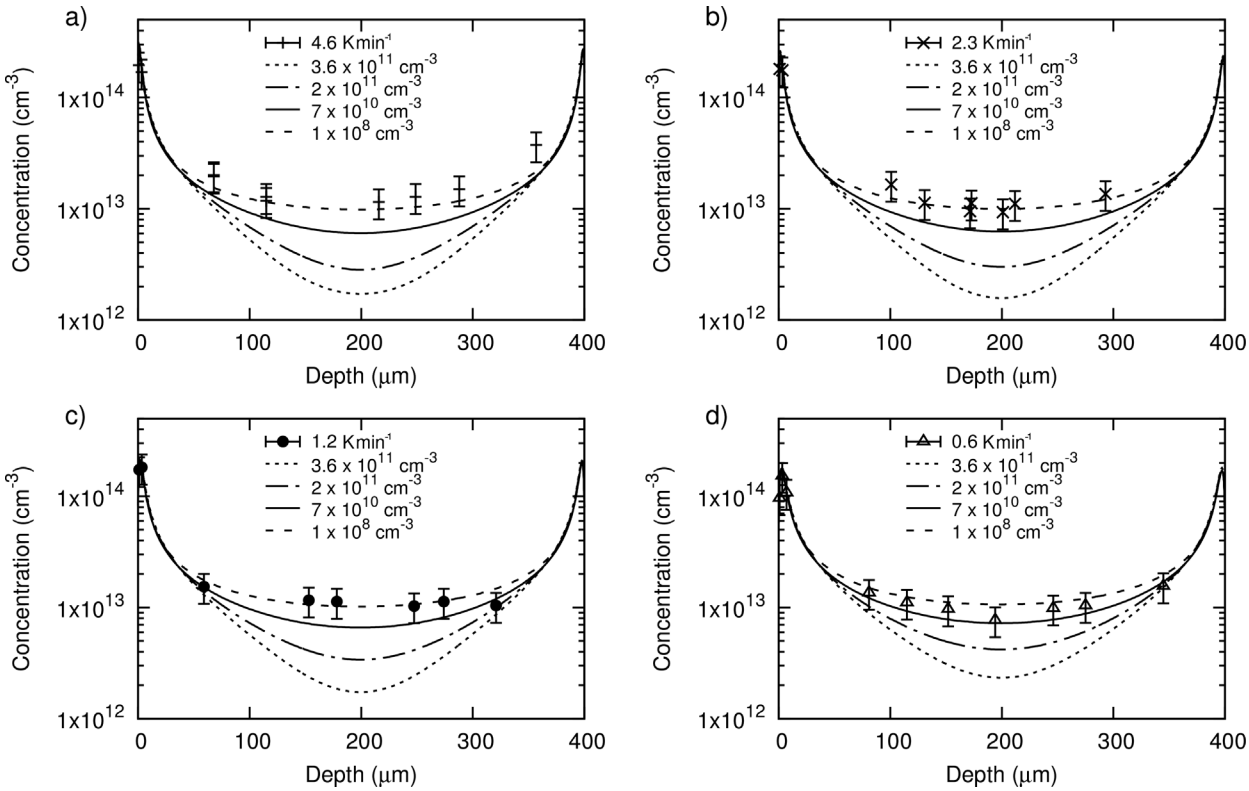


**Figure 2** DLTS measurements of the substitutional platinum concentration after annealing at 830 °C for 2 h followed by a ramping down of the temperature with ramping-down rates of a) + 4.6 K min$^{-1}$, b) × 2.3 K min$^{-1}$, c) • 1.2 K min$^{-1}$ and, d) △ 0.6 K min$^{-1}$). The points close to the surface are taken from Ref. [4]. The lines represent the simulation results for $C_I^{eq}$ at 830 °C of (· · ·) 3.6 ×10$^{11}$ cm$^{-3}$, (- — -) 2 ×10$^{11}$ cm$^{-3}$, (——) 7×10$^{10}$ cm$^{-3}$, and, (- - -) 1×10$^{8}$ cm$^{-3}$.

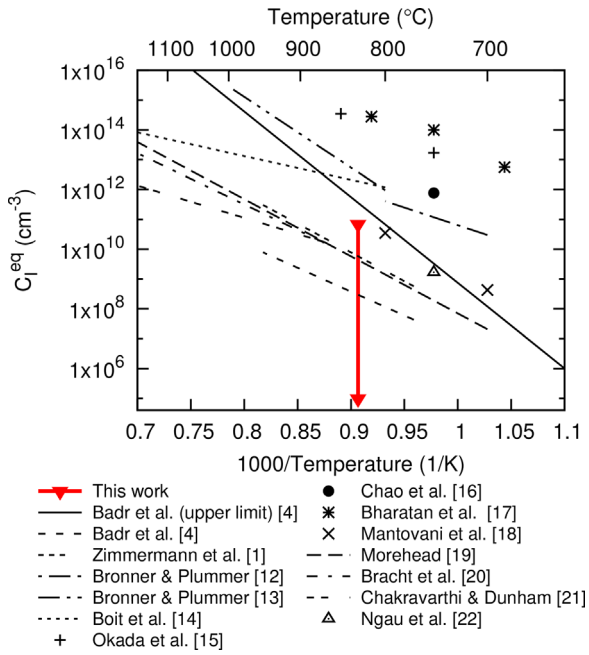


**Figure 3** Reported values for $C_I^{eq}$ compared to the upper limited at 830 °C determined in this work.

An upper limit for $C_I^{eq}$ at 830 °C was found by comparing simulations for increasing values to the measurements until the error margins of at least one of the measured profiles were significantly exceeded. The so determined upper limit of $7\times10^{10}$ cm$^{-3}$ predicts too low concentrations for ramping-down rates of 2.3 and 4.6 K min$^{-1}$ for all measured points in the bulk region, see Fig. 2a and b. Accordingly, our independently determined limit is lower by a factor of 5 than the $3.6\times10^{11}$ cm$^{-3}$ suggested by Badr et al. [4].

For the sake of completeness, an additional comment should be made with respect to the results for all ramping-down rates. The reaction rates become slower and slower with decreasing temperature. Accordingly, the time at higher temperatures becomes shorter for faster ramping-down rates. Finally, with increasing ramping-down rates, the limited time at higher temperatures will dynamically limit the reduction of $C_{Pt_s}$. Such an effect can be seen already for $C_I^{eq}(830\,°C) = 3.6\times10^{11}$ cm$^{-3}$, where the concentration in the bulk for 4.6 K min$^{-1}$ exceeds the one for 2.3 K min$^{-1}$ slightly, compare Fig. 2a and b.

**4.3 Comparison to other reported values** Figure 3 shows how the determined upper limit compares to other reported values of $C_I^{eq}$ at similar temperatures found in the literature. The compilation of values was taken from Ref. [5] and references therein, and from Badr et al. [4]. The high values from Refs. [12–17] are not compatible with our results. The values suggested in Refs. [1, 4, 18–22] are within our limits. Bracht et al. [20] and Chakravarthi and Dunham [21] deduced their expressions for $C_I^{eq}$ from the same Zn-diffusion experiments. In addition, Bracht et al. [20] also mentioned that a value of $C_I^{eq}$ which is greater by a factor of 5 failed to reproduce their measured results. The respective value of $4.28\times10^{10}$ cm$^{-3}$ at 830 °C is in good agreement with our upper limit.

**5 Conclusions** Experiments of platinum diffusion in silicon with annealing at a constant temperature for 2 h followed by a ramping down of the temperature with different rates were used to determine an upper limit for the equilibrium concentration of self-interstitials at 830 °C of about $7\times10^{10}$ cm$^{-3}$.

## References

[1] H. Zimmermann, Messung und Modellierung von Gold- und Platinprofilen, PhD Thesis, University of Erlangen-Nuremberg, (1991).
[2] M. Jacob, P. Pichler, H. Ryssel, and R. Falser, J. Appl. Phys. **82**, 182–191 (1997).
[3] F. Quast, Untersuchung von Punktdefekten inSilicium mit Hilfe der Platindiffusion, PhD Thesis, University of Erlangen-Nuremberg, (2001).
[4] E. Badr, P. Pichler, and G. Schmidt, J. Appl. Phys. **116**, 133508 (2014).
[5] P. Pichler, Intrinsic Point Defects, Impurities, and Their Diffusion in Silicon (Springer, Wien-New York, 2004), pp. 58–59 and pp. 136–140.
[6] F. C. Frank and D. Turnbull, Phys. Rev. **104** (3), 617–618, (1956).
[7] U. Gösele, W. Frank, and A. Seeger, Appl. Phys. **23** (4), 361–368, (1980).
[8] T. R. Waite, J. Chem. Phys. **94** (1), 103 (1958).
[9] P. Pichler, W. Jüngling, S. Selberherr, E. Guerrero, and H. W. Pötzl, IEEE Trans. Electron Devices **32**, 1940–1953, (1985).
[10] T. Südkamp and H. Bracht, Phys. Rev. B **94**, 125208 (2016).
[11] W. Lerch, N. A. Stolwijk, H. Mehrer, and C. Poisson, Semicond. Sci. Technol. **10**, 1257–1263, (1995).
[12] G. B. Bronner and J. D. Plummer, Appl. Phys. A. **36**, 49–54, (1985).
[13] G. B. Bronner and J. D. Plummer, J. Appl. Phys. **61** (8), 5536–5544, (1987).
[14] C. Boit, F. Lau, and R. Sittig, J. Electrochem. Soc. **50**, 197–205, (1990).
[15] T. K. Okada, H. Kawaguchi, S. Onaga, and K. Yamabe, in: 1991 International Workshop on VSLI Process and Device Modelling (1991 VPAD), (Japan Soc. of Appl. Phys.,1991), pp. 8–9.
[16] H. S. Chao, S. W. Crowder, P. B. Griffin, and J. B. Plummer, J. Appl. Phys. **79** (5), 2352–2363 (1996).
[17] S. Bharatan, Y. M. Haddara, M. E. Law, and K. S. Jones, MRS Proceedings **532**, 111–118, (1998).
[18] S. Mantovani, F. Nava, C. Nobili, and G. Ottaviani, Phys. Rev. B **33** (8), 5536–5544, (1986).
[19] F. F. Morehead, Mat. Res. Soc. Symp. Proc. **104**, 99–104, (1988).
[20] H. Bracht, N. A. Stolwijk, and H. Mehrer, Phys. Rev. B. **52** (23), 16542–16560 (1995).
[21] S. Chakravarthi and S. T. Dunham, Mat. Res. Soc. Symp. Proc. **469**, 47–52 (1997).
[22] J. L. Ngau, P. B. Griffin, and J. D. Plummer, J. Appl. Phys. **90** (4), 1768–1778, (2001).

 